2. Results

2.1 Tyrosine phosphorylation of phospholipase D1

Evidence for regulation of phospholipase D by tyrosine phosphorylation was concluded from the fact that phospholipase D activity can be induced by epidermal growth factor and platelet derived growth factor (Ben-Av *et al.*, 1989; Fisher *et al.*, 1991). Moreover, induction of phospholipase D activity by hydrogen peroxide in neutrophils can be abolished by tyrosine kinase inhibitors. Using the protein tyrosine phosphatase inhibitor pervanadate Bourgoin and Grinstein (1992) could show enhanced phospholipase D activity in HL60 cells and later tyrosine phosphorylation of phospholipase D1 (Marcil *et al.*, 1997).

In order to investigate a possible role of tyrosine phosphorylation in the regulation of phospholipase D1 activity in HaCaT keratinocytes, serum-induced cells were treated with sodium pervanadate. Postconfluent cells were serum starved for 24 h. Prior to addition of sodium pervanadate, the cells were incubated with serum-containing medium for 5 min at 37 °C. After incubation in the presence of 100 μM hydrogen peroxide or 100 μM sodium pervanadate for 10 min at 37 °C the cells were lysed. Lysates were subjected to SDS-PAGE and subsequently transferred to nitrocellulose. Western blot analysis with the monoclonal anti phosphotyrosine antibody PY-20 showed an increase in tyrosine phosphorylated proteins in HaCaT cells after treatment with sodium pervanadate (Fig. 5). Preincubation for 5 min with 1 mM genistein completely abolished tyrosine phosphorylation, whereas 100 nM staurosporine had no effect. Preincubation with 100 nM 12-*O*-tetradecanoyl phorbol-13-acetate (TPA) or 30 μM *N*-acetyl-D-sphingosine (C_2-Ceramide) enhanced tyrosine phosphorylation in HaCaT cells.

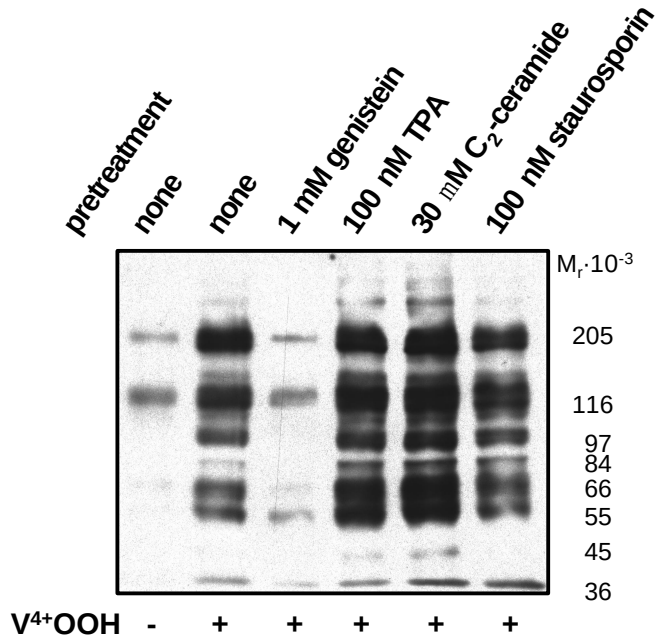

Figure 5:
Tyrosine phosphorylation in serum induced HaCaT cells using sodium pervanadate ($V^{4+}OOH$). Cells were serum-starved for 24 h and 5 min prior to addition of $V^{4+}OOH$ supplemented with fresh medium containing indicated agents. After application of 100 µM hydrogen peroxide (-) or 100 µM $V^{4+}OOH$ (+) the cells were further incubated for 10 min at 37 °C. Cell lysates, 40 µg each were separated on a 10 % SDS-PAGE and transferred to nitrocellulose. The membrane was probed with anti phosphotyrosine antibodies PY-20 and detected using SuperSignal chemiluminescence reagent.

The activity of phospholipase D1 was determined in *in vitro* assays with lysates of sodium pervanadate treated cells. For this purpose, the transphosphatidylation activity of the enzyme was exploited. In this reaction the non-physiologic product phosphatidylethanol is generated if ethanol is present as a substrate. Phospholipase D1 has an absolute requirement for phosphatidylinositol-4,5-bisphosphate (PIP_2) and is activated by monomeric G-proteins. Therefore, phospholipase D activity was measured with substrate vesicles containing phosphatidylethanolamine (PE), PIP_2 and phosphatidylcholine (PC) at a ratio of 18:1.4:1 (w/w/w) with 8.6 µM PC, 100 µM guanosine-5'-*O*-(3-thiotriphosphate) (GTPγS) and 0.4 µg/µl protein for 1 h at 37 °C. Phospholipase D1 activity was significantly increased in sodium pervanadate treated HaCaT cells as well as in Ras transfected HaCaT cells or HL60 cells (Fig. 6). This increase could be completely blocked by pretreatment with 1 mM genistein in all three cell lines tested. Sodium vanadate at 100 µM or 1 mM genistein added directly to the assay had no effect on phospholipase D activity *in vitro* suggesting a tyrosine phosphorylation dependent activation of phospholipase D1 in these cells. In fact, vanadate is a potent inhibitor of phospholipase D from peanut as well as of human phospholipase D1 overexpressed in *Spodoptera frugiperda* insect cells at higher concentrations (data not shown).

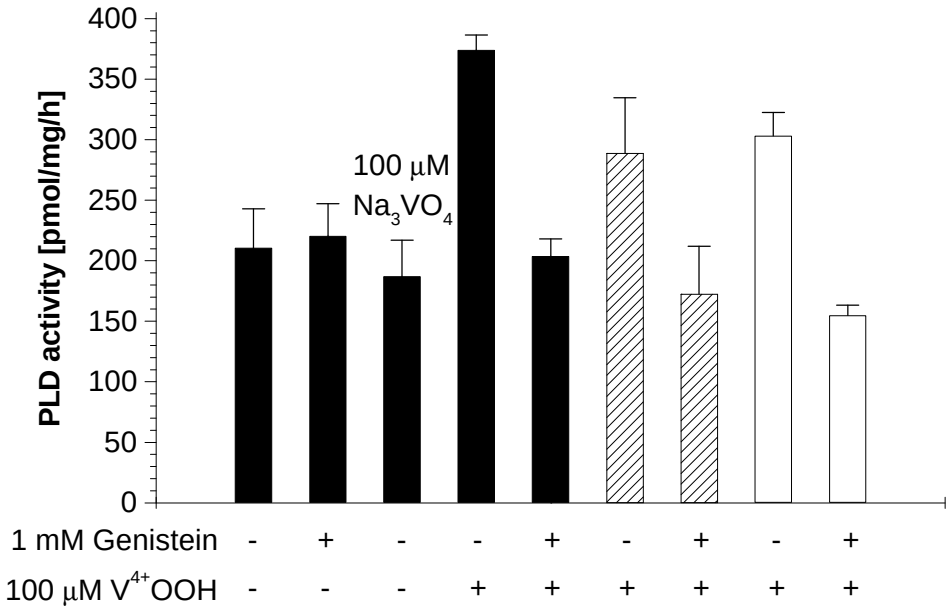

Figure 6:
Induction of phospholipase D1 activity by tyrosine phosphorylation. Cells were serum-starved for 24 h and 5 min prior to addition of sodium pervanadate ($V^{4+}OOH$) supplemented with DMSO or 1 mM genistein as indicated. After application of 100 μM $V^{4+}OOH$ the cells were further incubated for 10 min at 37 °C. Phospholipase D1 activity was determined *in vitro* by phosphatidylethanol generation. The assay contained 0.4 μg/μl protein and 100 μM guanosine-5'-*O*-(3-thiotriphosphate). Solid bars represent HaCaT cells, hatched bars ras-transfected HaCaT cells and clear bars HL60 cells. Error bars represent the standard deviation for three independent experiments.

Immunoprecipitation was used to investigate direct tyrosine phosphorylation of phospholipase D1 in HaCaT keratinocytes, Ras transfected HaCaT keratinocytes and HL60 cells. Lysates of cells treated with sodium pervanadate, pretreated or untreated with 1 mM genistein, were precipitated with anti hPLD1 antibody (αNChPLD1) on protein A-sepharose. Precipitates were subjected to SDS-PAGE and subsequently transferred to nitrocellulose. Western blot was performed with anti phosphotyrosine antibody PY-20 (Fig. 7). In contrast to HL60 cells, HaCaT cells and Ras transfected HaCaT cells did not show any tyrosine phosphorylated band in immunoprecipitates. Inhibition of tyrosine dephosphorylation was proven by Western blot of supernatants using PY-20 (data not shown). Only HL60 cells showed a band with a molecular weight of $M_r = 110 \cdot 10^3$, which is lacking in genistein pretreated cells, correlating to tyrosine phosphorylated hPLD1. The membrane was stripped using low pH and sodium azide to destroy peroxidase activity. The blot was reprobed with αNChPLD1 antibodies and showed a strong band with a molecular weight of $M_r = 110 \cdot 10^3$ for all precipitates. The weaker band for treated HL60 cells results from incomplete stripping of the PY-20 antibodies.

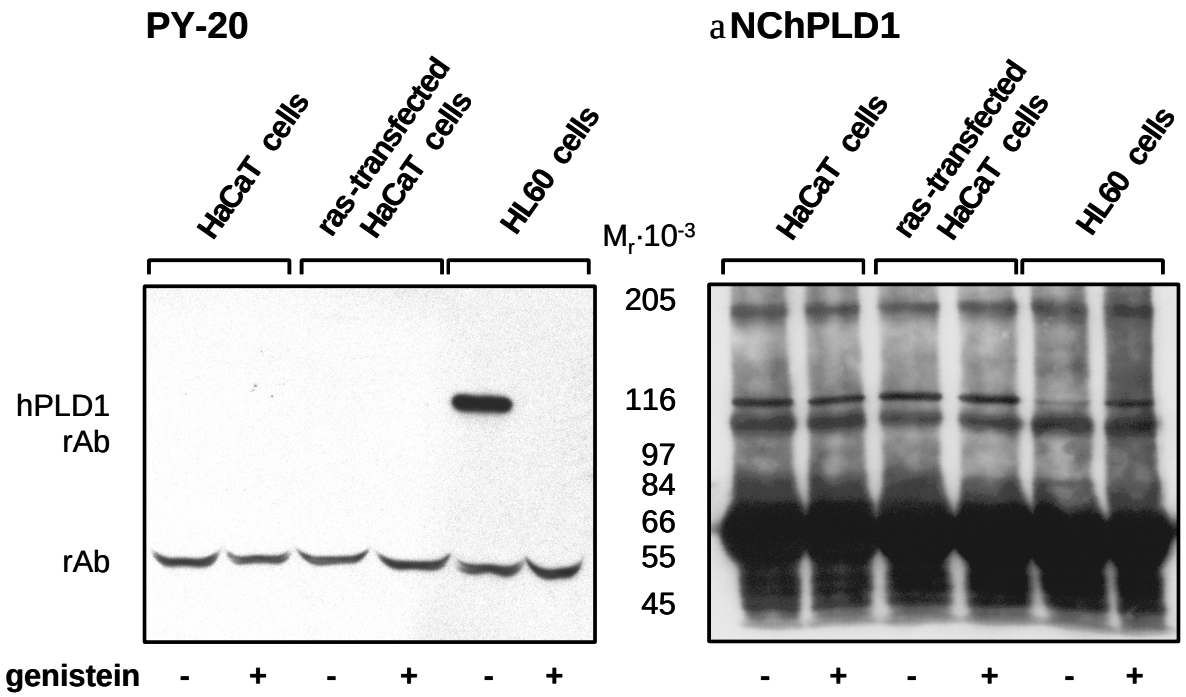

Figure 7:
Tyrosine phosphorylation of hPLD1 in serum induced cells using sodium pervanadate ($V^{4+}OOH$). Cells were serum-starved for 24 h and 5 min prior to addition of $V^{4+}OOH$ supplemented with fresh medium containing DMSO or 1 mM genistein. After application of 100 μM $V^{4+}OOH$ the cells were further incubated for 10 min at 37 °C. Cell lysates, 800 μg each were precipitated using αNChPLD1 antibodies with protein A-sepharose. The precipitates were separated on a 6 % SDS-PAGE and transferred to nitrocellulose. The membrane was probed with anti phosphotyrosine antibodies PY-20 and after stripping with αNChPLD1 antibodies. Detection was achieved using SuperSignal chemiluminescence reagent. rAb, rabbit antibody.

Additionally, in immunoprecipitates of [^{32}P]-phosphate labelled cells no phosphorylation of hPLD1 in HaCaT keratinocytes could be detected (data not shown).

2.2 Expression of phospholipase D and differentiation-associated genes in ceramide induced apoptosis in HaCaT keratinocytes

Ceramides were shown to have a direct as well as an indirect negative effect on phospholipase D activities (ABOUSALHAM *et al.*, 1997; YOSHIMURA *et al.*, 1997). In keratinocytes, ceramide induced apoptosis shows features of keratinocyte differentiation like cornified envelope formation (WAKITA *et al.*, 1994). In my diploma thesis, I could show a correlation of phospholipase D levels and keratinocyte growth. To distinguish whether ceramide-induced apoptosis parallels differentiation, the transcription of keratinocyte differentiation-associated genes after stimulation with ceramide was investigated.

HaCaT cells grown in KGM to 80 % confluence were treated for 2 h, 6 h and 24 h with 30 μM C_2-ceramide or ethanol as vehicle control. Subsequently, total RNA was isolated and cDNA synthesis with 2 μg of RNA performed. The obtained cDNA was used for PCR under

conditions specific for the particular primer pair (see chapter 5.6). Primer pairs were designed using MacMolly Tetra (Softgene, Berlin, D) software with the following parameters.

The 5'- and 3'-primer sequences were chosen to be localised within two different exons when intron-exon boundaries were known. Amplification of DNA contamination will thus result in longer amplicons due to inclusion of introns. The isoform-distinguishing primers for *phospholipase D1* were designed so that the *phospholipase D1a* 5'-primer sequence lies inside the alternatively spliced exon and the *phospholipase D1b* 5'-primer sequence encompasses the splice site. The same 3'-primer was used for both the *phospholipase D1a* and *phospholipase D1b* PCR. Furthermore, identical annealing temperatures as computed by the software were chosen for a primer pair. Complementarity within a primer or a primer pair was as low as possible. PCR protocols were optimised so that the product is received in the phase of exponential amplification.

Reaction products were separated on 2 % agarose gels stained with ethidium bromide and scanned using video densitometry. For semi-quantitative analysis, three independent experiments were performed in duplicate. The intensity of each band was analysed using MultiAnalyst (BioRad, Munich, D) software and the mean value of duplicate experiments normalised using the mean value of the respective *ribo S9* experiments. The median of three independent experiments of treatment with C_2-ceramide was then set relative to the respective treatment with ethanol. The results are shown in figure 8.

The mRNA of the constituents of the transcription factor AP-1, *c-jun* and *fosB* are upregulated eight- and fourfold after 24 h of C_2-ceramide treatment, respectively. However, another constituent of AP-1, *c-fos* shows a transient upregulation after 6 h but normal levels after 24 h. Tissue transglutaminase is activated during apoptosis. Its mRNA levels are not significantly altered by treatment with C_2-ceramide. The four keratinocyte differentiation-associated genes *involucrin*, *loricrin*, *keratin V* and *transglutaminase 1* are all downregulated after 24 h of treatment with C_2-ceramide. Similarly, the transcripts of *phospholipase D1a* and *phospholipase D1b* are both downregulated after 24 h of treatment with C_2-ceramide whereas *phospholipase D2* shows no change of mRNA levels.

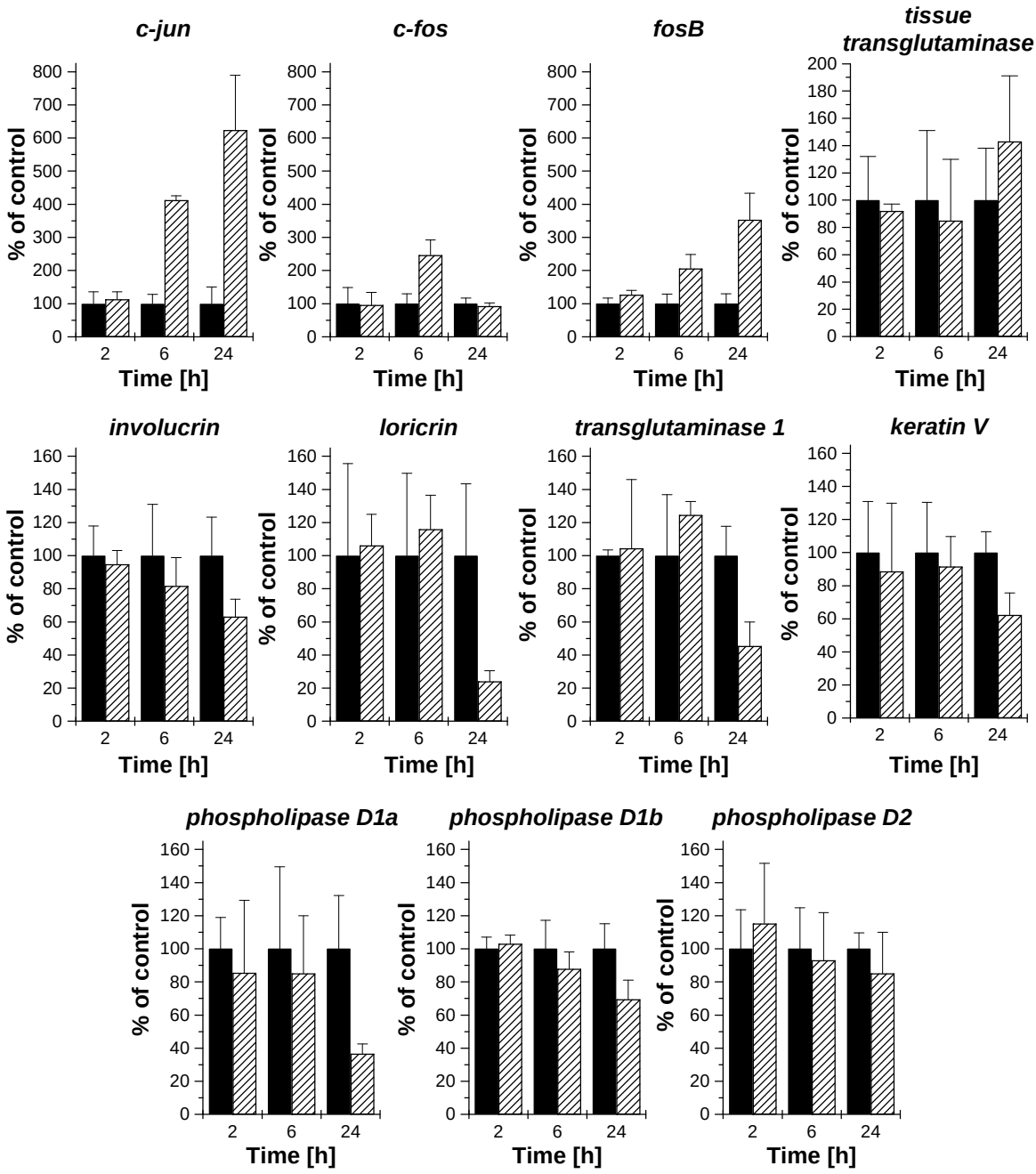

Figure 8:
Gene expression in ceramide induced apoptosis in HaCaT cells. Cells of 80 % confluence were treated with 30 μM *N*-acetyl-D-sphingosine (C_2-ceramide; hatched bars) or ethanol (vehicle; solid bars) for indicated times. Total RNA was isolated, cDNA synthesis with 2 μg of RNA performed and PCR with primers specific for the indicated mRNA was carried out. PCR products were separated on 2 % agarose gels and analysed using video densitometry. Error bars represent the standard deviation for three independent experiments.

2.3 Expression of phospholipase D and its stimulatory proteins in human melanoma cells and primary cultured melanocytes

To investigate the expression of phospholipase D isoforms in melanoma cells and primary cultured melanocytes, total RNA was isolated from post confluent grown cells. Synthesis of cDNA with 2 µg of total RNA was followed by PCR using specific primers under appropriate conditions (see chapter 5.6). Primers were designed and protocols optimised as described in chapter 2.2. Figure 9 shows the reaction products separated on 2 % agarose gels stained with ethidium bromide and scanned using video densitometry.

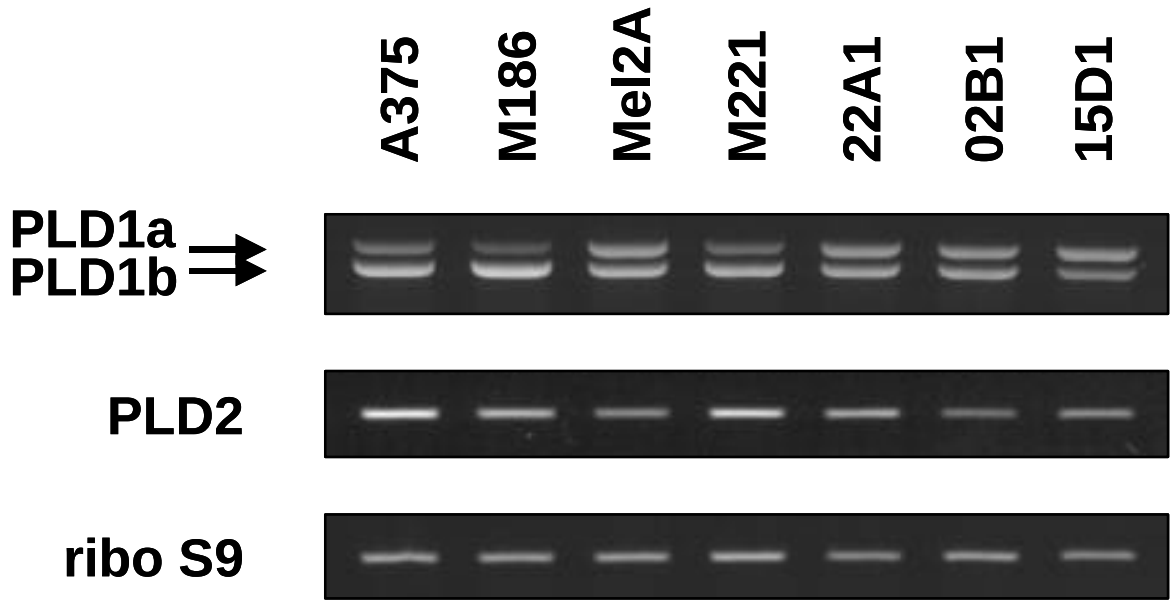

Figure 9:
Expression of phospholipase D isoforms in melanoma cells and melanocytes. Total RNA was isolated from post confluent grown cells, cDNA synthesis with 2 µg of RNA performed and PCR with primers specific for the indicated mRNA was carried out. PCR products, 10 µl each were separated on 2 % agarose gels and visualised using ethidium bromide staining. PLD1a, PLD1b, phospholipase D1 splicing isoforms a and b, respectively; PLD2, phospholipase D2; ribo S9, ribosomal protein S9. A375, M186, Mel2A and M221 are melanoma cells; 22A1, 02B1 and 15D1 were primary cultured melanocytes.

Using a primer pair encompassing the alternatively spliced exon of *phospholipase D1*, it appears that all investigated cell lines express both splicing isoforms. Whereas Mel2A cells and primary human melanocytes express both isoforms in equal amounts, A375, M186 and M221 express more *phospholipase D1b* than *phospholipase D1a*. This primer pair also encompasses a putative *phospholipase D1c* isoform that completely lacks the loop region, resembling in this respect *phospholipase D2*. With cDNA from U937 cells, which lack expression of phospholipase D2, a faint band of the correct size was seen but no expression was seen in the other cell lines tested (data not shown). The second gene of this phospholipase D family, *phospholipase D2* is expressed at high levels in A375 and M221 cells but at

moderate levels in M186, Mel2A and the three melanocyte cultures 22A1, 02B1 and 15D1. The expression of *ribosomal protein S9* was included to show that comparable amounts of RNA were used.

The expression of phospholipase D and its stimulatory proteins was examined using Western blot. Whole cell lysates were prepared from post confluent grown cells and subjected to SDS-PAGE. Subsequently, the gels were transferred to nitrocellulose membranes and the membranes probed with specific antibodies. The resulting immunocomplexes were detected using chemiluminescence.

The four melanoma cell lines A375, M186, Mel2A and M221 showed equal amounts of phospholipase D1 whereas the band was very weak in melanocytes (Fig. 10). PKCα is expressed throughout the investigated cells with Mel2A showing low levels. RhoA showed high expression in primary human melanocytes, moderate expression in M186, Mel2A and M221, but only weak expression in A375. However, ADP-ribosylation factor proteins are strongly expressed in A375, but weak in M186, Mel2A and M186. No ADP-ribosylation factor proteins could be detected using whole cell lysates in primary human melanocytes. Western blot with anti actin antibodies was included to show that comparable amounts of protein were used.

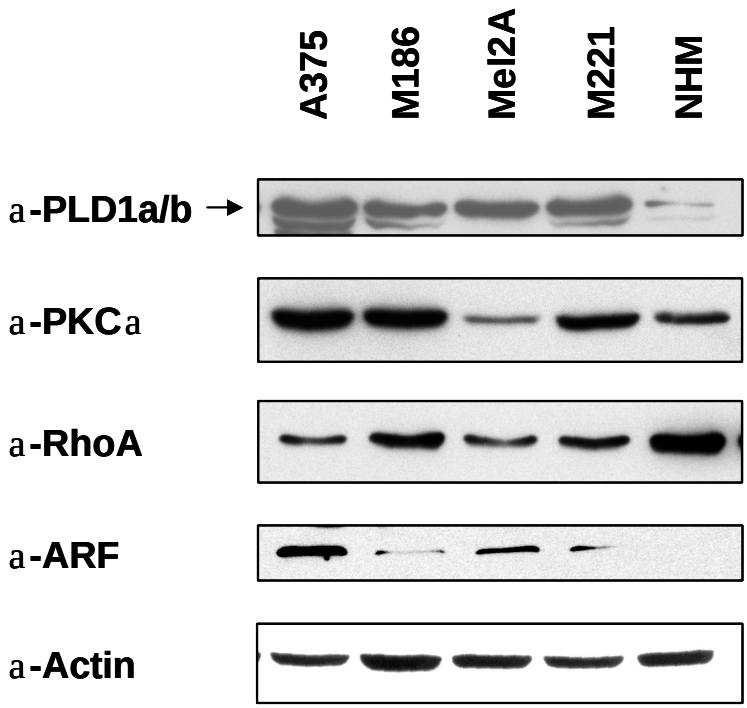

Figure 10:
Expression of phospholipase D and stimulatory proteins in melanoma cells and melanocytes. Whole cell lysates were prepared from post confluent grown cells and 50 μg of each were separated on 6 % SDS-PAGE (α-PLD1a/b and α-PKCα) or 15 % SDS-PAGE (α-RhoA and α-ARF). After transfer to nitrocellulose the membrane was probed with the indicated antibodies. Immunocomplexes were detected using SuperSignal chemiluminescence reagent. A375, M186, Mel2A and M221 are melanoma cells, NHM were primary cultured melanocytes.

The subcellular localisation of phospholipase D was examined using the alkaline phosphatase anti alkaline phosphatase (APAAP) technique. Cells were grown on chamber slides and fixed with acetone. The slides were then incubated with αNChPLD1 and subsequently alkaline phosphatase anti alkaline phosphatase antibodies. The resulting immunocomplexes were detected using new fuchsin (red) and the nucleus was counterstained using hematoxilin (blue).

Figure 11 shows a representative picture of A375 cells. The staining is cytosolic and no dyeing is seen inside the nucleus (N). In the most cases the staining is strongest around the nucleus. Additionally, some cells exhibit staining of restricted membrane regions.

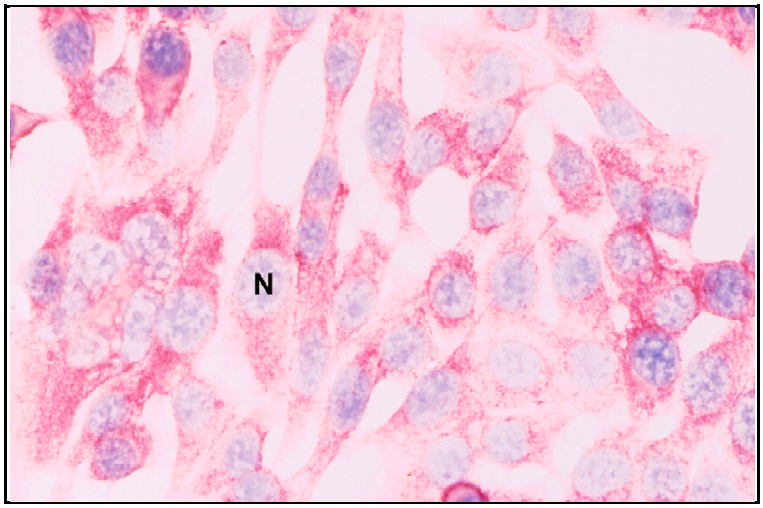

Figure 11: Immunohistochemical detection of phospholipase D in A375 melanoma cells. Cells were grown on chamber slides, fixed in acetone and processed using αNChPLD1 antibodies and the alkaline phosphatase anti alkaline phosphatase antibody (APAAP) technique. The preparations were photographed using an 1:40 objective.

2.4 Effect of phorbol ester and guanosine-5'-*O*-(3-thiotriphosphate) on phospholipase D in melanoma cells

HAMMOND *et al.* (1997) showed that human phospholipase D1a and phospholipase D1b can be activated *in vitro* by protein kinase C, ADP-ribosylation factor and Rho family proteins using proteins overexpressed in *Spodoptera frugiperda* insect cells and that this activation is synergistic. On the contrary, PARK *et al.* (1997) showed that rat phospholipase D1b is activated by the same proteins, but found no synergism.

The activity of phospholipase D1 was determined in *in vitro* assays with lysates of post confluent grown cells. For this purpose, the transphosphatidylation activity of the enzyme generating the nonphysiologic product phosphatidylethanol if ethanol was present as a substrate is exploited. Phospholipase D1 has an absolute requirement for phosphatidylinositol-4,5-bisphosphate (PIP_2). Therefore, phospholipase D activity was measured with substrate vesicles containing phosphatidylethanolamin (PE), PIP_2 and phosphatidylcholine (PC)

18:1.4:1 (w/w/w) with 8.6 µM PC, 0.8 µg/µl protein and guanosine-5'-*O*-(3-thiotriphosphate) (GTPγS) and 12-*O*-tetradecanoyl phorbol-13-acetate (TPA) as indicated for 1 h at 37 °C.

Varying the concentration of TPA in the absence of GTPγS shows a concentration dependent increase of phospholipase D activity with an EC_{50} of about 20 nM (Fig. 12).

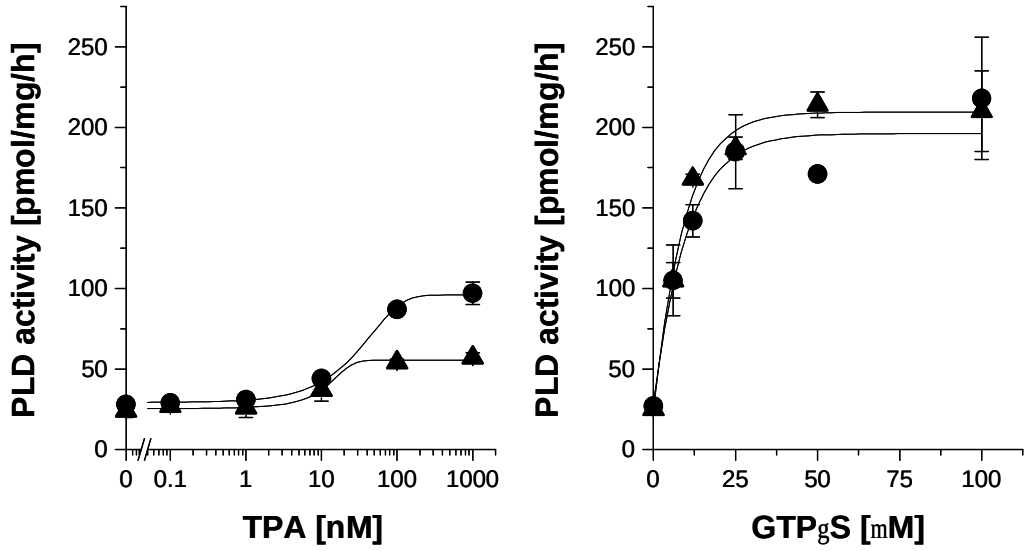

Figure 12:
Dependency of phospholipase D activity on 12-*O*-tetradecanoyl phorbol-13-acetate (TPA) and guanosine-5'-*O*-(3-thiotriphosphate) (GTPgS) in melanoma cells. Whole cell lysates were prepared from post confluent grown A375 (circles) and Mel2A (triangles) melanoma cells. Phospholipase D1 activity was determined *in vitro* by phosphatidylethanol generation. The assay contained 0.4 µg/µl protein and TPA or GTPγS as indicated. Error bars represent the standard deviation for three independent experiments.

Maximal activation was 3.1- and 2.3-fold at 100 nM TPA for A375 and Mel2A, respectively. Using increasing concentrations of GTPγS in the absence of TPA also showed a concentration dependent stimulation of phospholipase D activity. The EC_{50} for GTPγS was 12 µM and maximal activation was about sevenfold at 50 µM GTPγS for both cell lines. Combining both stimuli at 100 nM TPA and 50 µM GTPγS yielded phospholipase D activities of 15-fold, 17-fold, 20-fold and 22-fold above basal for A375, M186, Mel2A and M221, respectively (Fig. 13). Absolute activities for each stimulus were at comparable levels in all melanoma cell lines tested. Depleting the cells from protein kinase C by treatment with 100 nM TPA in serum-free medium for 24 h resulted in a complete loss of the TPA response of phospholipase D activity and also no synergism was seen in combination with 50 µM GTPγS (Fig. 14).

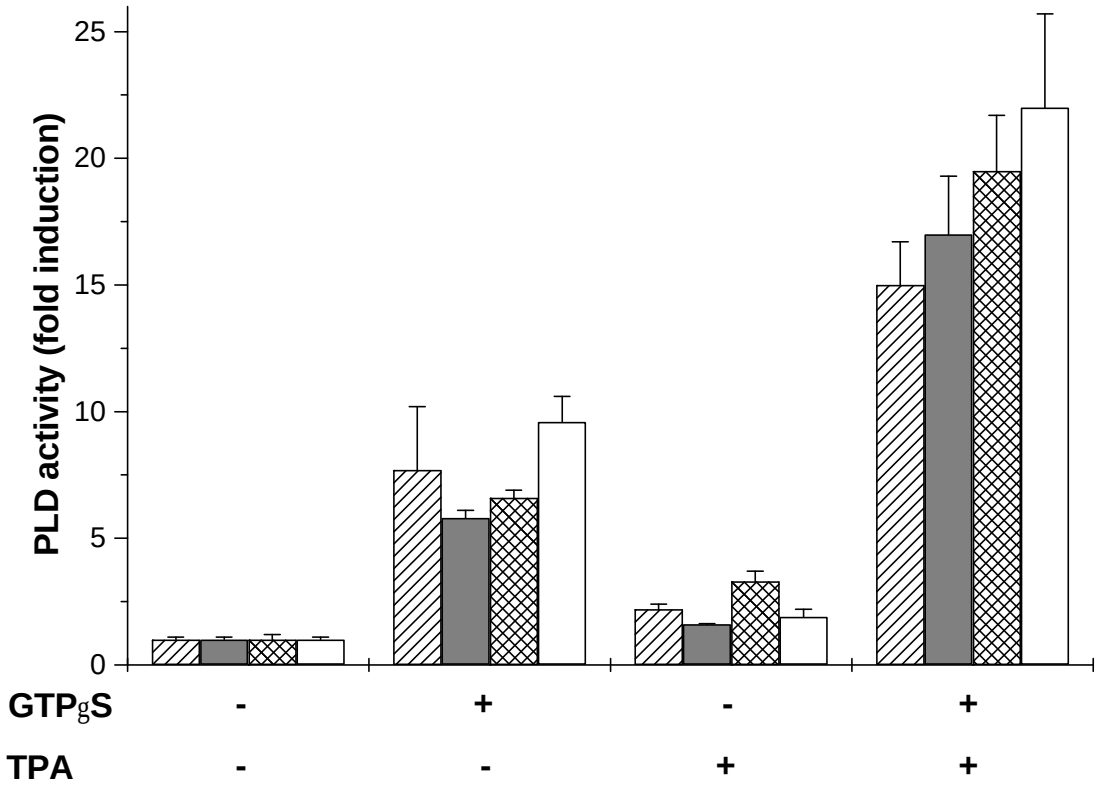

Figure 13:
Synergism of 12-*O*-tetradecanoyl phorbol-13-acetate (TPA) and guanosine-5'-*O*-(3-thiotriphosphate) (GTPgS) on phospholipase D activity in melanoma cells. Whole cell lysates were prepared from post confluent grown A375 (hatched bars), M186 (grey bars), Mel2A (crossed bars) and M221 (white bars) melanoma cells. Phospholipase D1 activity was determined *in vitro* by phosphatidylethanol generation. The assay contained 0.4 μg/μl protein and 100 nM TPA and 50 μM GTPγS as indicated. Error bars represent the standard deviation for three independent experiments.

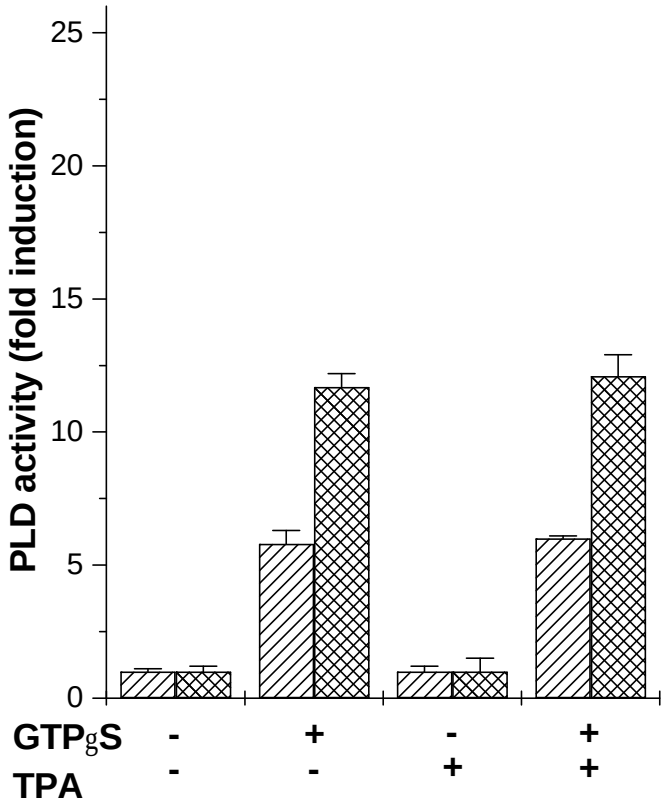

Figure 14:
Effect of protein kinase C depletion on the synergism of 12-*O*-tetradecanoyl phorbol-13-acetate (TPA) and guanosine-5'-*O*-(3-thiotriphosphate) (GTPgS) on phospholipase D activity in melanoma cells. Post confluent grown A375 (hatched bars) and Mel2A (crossed bars) melanoma cells were serum-starved for 24 h in the presence of 100 nM TPA and whole cell lysates were prepared. Phospholipase D1 activity was determined *in vitro* by phosphatidylethanol generation. The assay contained 0.4 µg/µl protein and 100 nM TPA and 50 µM GTPγS as indicated. Error bars represent the standard deviation for three independent experiments.

In contrast, absolute phospholipase D1 activities of primary cultured melanocytes were lower than in A375 melanoma cells (Fig. 15). Whereas A375 melanoma cells exhibit a phospholipase D1 activity of (221 ± 45) pmol/mg/h when stimulated with 50 µM GTPγS, melanocytes produced (65 ± 17) pmol/mg/h phosphatidylethanol under the same conditions. Therefore, phospholipase D1 activity was induced about ninefold in A375 and fourfold in melanocytes. While 100 nM TPA stimulated phospholipase D activity twofold in A375 it was 1.4-fold elevated in melanocytes. Moreover, no synergism was observed using TPA and GTPγS in combination in melanocytes in contrast to A375 melanoma cells.

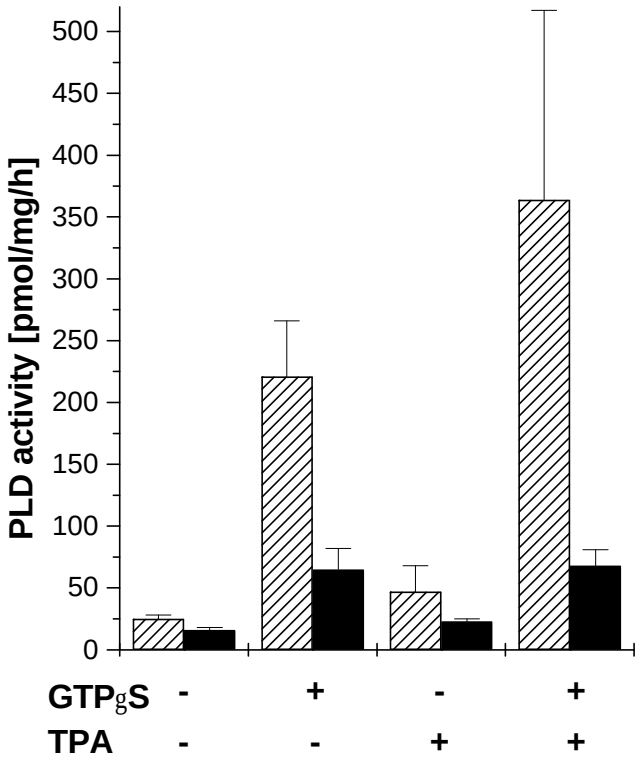

Figure 15:
Synergism of 12-*O*-tetradecanoyl phorbol-13-acetate (TPA) and guanosine-5'-*O*-(3-thiotriphosphate) (GTP$_g$S) on phospholipase D activity in primary cultured melanocytes. Whole cell lysates were prepared from post confluent grown A375 (hatched bars) and primary cultured melanocytes (black bars). Phospholipase D1 activity was determined *in vitro* by phosphatidylethanol generation. The assay contained 0.4 μg/μl protein and 100 nM TPA and 50 μM GTPγS as indicated. Error bars represent the standard deviation for three independent experiments.

2.5 Effect of oleate on phospholipase D in melanoma cells

Besides phospholipase D1 and phospholipase D2 a phosphatidylcholine-specific phospholipase D activity is described for mammalian cells that is activated by millimolar concentrations of oleate. In contrast, phospholipase D1 is strongly inhibited by oleate and phospholipase D2 is claimed to be activated by micromolar concentrations of oleate but also inhibited using millimolar concentrations.

Using PIP_2 containing substrate vesicles with 100 nM TPA and 50 μM GTPγS, phospholipase D activity was strongly inhibited by oleate with an IC_{50} of about 40 μM (Fig. 16). Phospholipase D activity was completely abolished at 0.5 mM oleate. However, the corresponding saturated fatty acylate stearate inhibited phospholipase D activity with an IC_{50} of 1.2 mM and is therefore a 30-fold less potent inhibitor.

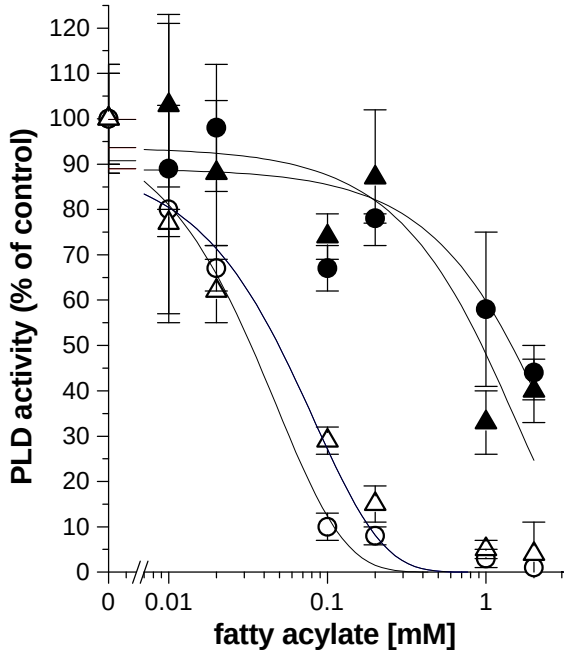

Figure 16:
Effect of oleate on phospholipase D activity in melanoma cells. Whole cell lysates were prepared from post confluent grown A375 (circles) and Mel2A (triangles) melanoma cells. Phospholipase D1 activity was determined *in vitro* by phosphatidylethanol generation. The assay contained 0.4 μg/μl protein, 100 nM TPA, 50 μM GTPγS and sodium stearate (solid symbols) or sodium oleate (open symbols) as indicated. Error bars represent the standard deviation for three independent experiments.

2.6 Effect of pamidronate on melanoma cells

Pamidronate is a bisphosphonate acting as non-hydrolysable pyrophosphate analogue. Nitrogen containing bisphosphonates like pamidronate were shown to inhibit the farnesyl diphosphate synthase (VAN BEEK *et al.*, 1999). They are therefore inhibitors of the synthesis of higher isoprenoids. The main isoprenoid affected is geranylgeranyl diphosphate which is used in the prenylation of monomeric G-proteins of the Ras superfamily like Rho proteins. Geranylgeranylation of these proteins is required for their membrane association and hence, activity.

To investigate the effect of pamidronate on viability, melanoma cells of 40 % confluency were treated with pamidronate at different concentrations for 48 h. The cell number of adhering cells was examined using the crystal violet staining of nuclei. After washing, the bound crystal violet was released using Triton X-100 and its quantity analysed with an ELISA photometer. The absorption of vehicle-treated cells was set to 100 % and treated cells were expressed as percent of control. Treatment with pamidronate resulted in significantly decreased cell numbers in A375, M186 and M221, but not in Mel2A (Fig. 17). Inhibition of proliferation reached its maximum at 100 μM pamidronate with (83 ± 4) % of control for A375, (89 ± 4) % of control for M186 and (76 ± 4) % of control for M221. Higher concentrations of 250 μM pamidronate did not further reduce cell numbers.

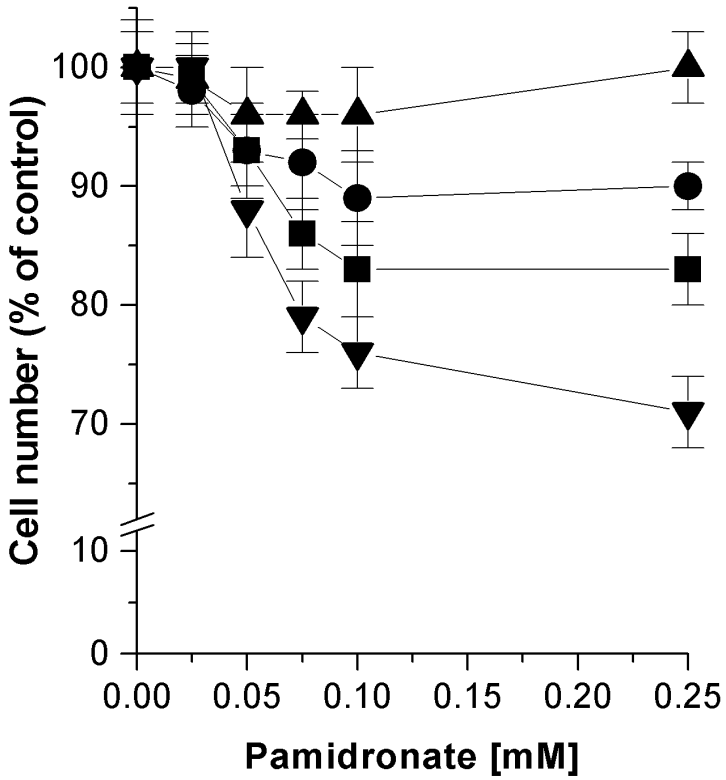

Figure 17:
Effect of pamidronate on melanoma cell proliferation. Melanoma cells of 40 % confluency were treated with indicated concentrations of pamidronate or vehicle control for 48 h. Proliferation was measured using crystal violet staining of adherent cells. Squares, A375; circles, M186; up triangles, Mel2A; down triangles, M221. Error bars represent the standard deviation for four independent experiments.

A possible unspecific cytotoxic effect of pamidronate was examined by release of lactate dehydrogenase into the cell culture supernatant. Lactate dehydrogenase is a cytosolic enzyme that is released upon membrane disruption as a typical feature of cytotoxicity. Melanoma cells of 80 % confluency were treated with pamidronate at different concentrations for 24 h. Lactate dehydrogenase activity was assessed using an chromogenic substrate and analysed with an ELISA photometer. The absorption of vehicle-treated cells was set to 100 % and treated cells were expressed as percent of control. No significant increase of lactate dehydrogenase activity in cell culture supernatants was observed following treatment with pamidronate for the cell lines tested (Fig. 18).

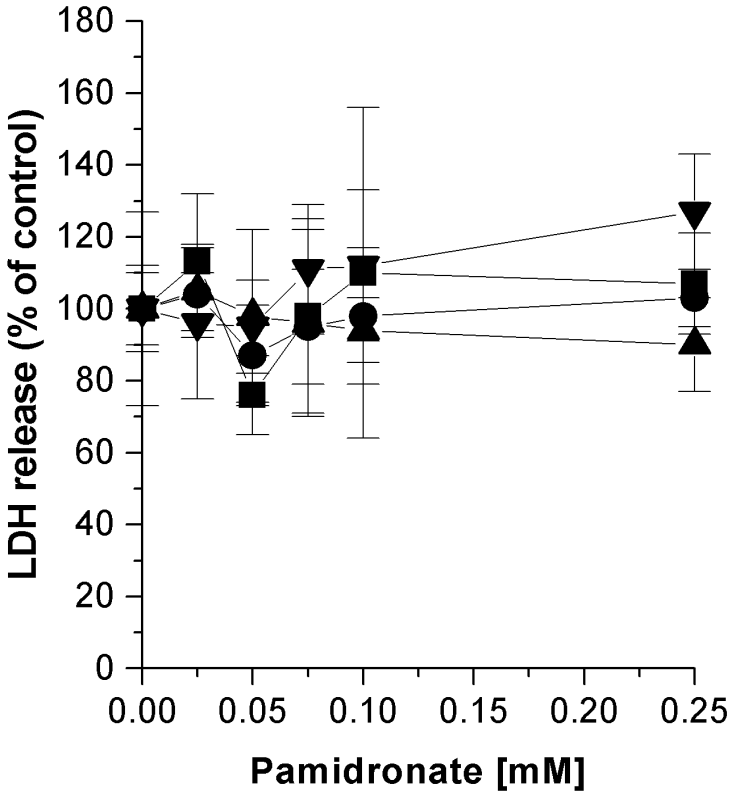

Figure 18:
Cytotoxicity of pamidronate on melanoma cells. Melanoma cells of 80 % confluency were treated with indicated concentrations of pamidronate or vehicle control for 24 h. Cytotoxicity was measured as release of lactate dehydrogenase activity in the cell culture supernatant. Squares, A375; circles, M186; up triangles, Mel2A; down triangles, M221. Error bars represent the standard deviation for four independent experiments.

Apoptosis is a controlled form of cell death. One of its features is the degradation of nuclear DNA resulting in histone-bound DNA fragments released into the cytosol of the cell. Melanoma cells of 80 % confluency were treated with pamidronate at different concentrations for 24 h. Cytosolic extracts were incubated with antibodies against DNA and antibodies against histones. The anti DNA antibodies are used to immobilise the complex and the anti histone antibodies are coupled to peroxidase. Latter can be assessed using a chromogenic substrate with an ELISA photometer. The absorption of vehicle-treated cells was set to 100 % and treated cells were expressed as percent of control. Treatment with pamidronate resulted in significantly increased apoptosis in A375, M186 and M221 but not in Mel2A (Fig. 19). Apoptosis was observed at 50 μM pamidronate with (433 ± 31) % of control for A375, (134 ± 1) % of control for M186 and (129 ± 6) % of control for M221. Apoptosis reached its maximum at 100 μM pamidronate with (997 ± 35) % of control for A375, (154 ± 5) % of control for M186 and (162 ± 16) % of control for M221. Higher concentrations of 250 μM pamidronate did not further enhance DNA fragmentation. At concentrations of 500 μM and 1 mM, pamidronate precipitates and induction of apoptosis is strongly reduced (data not shown).

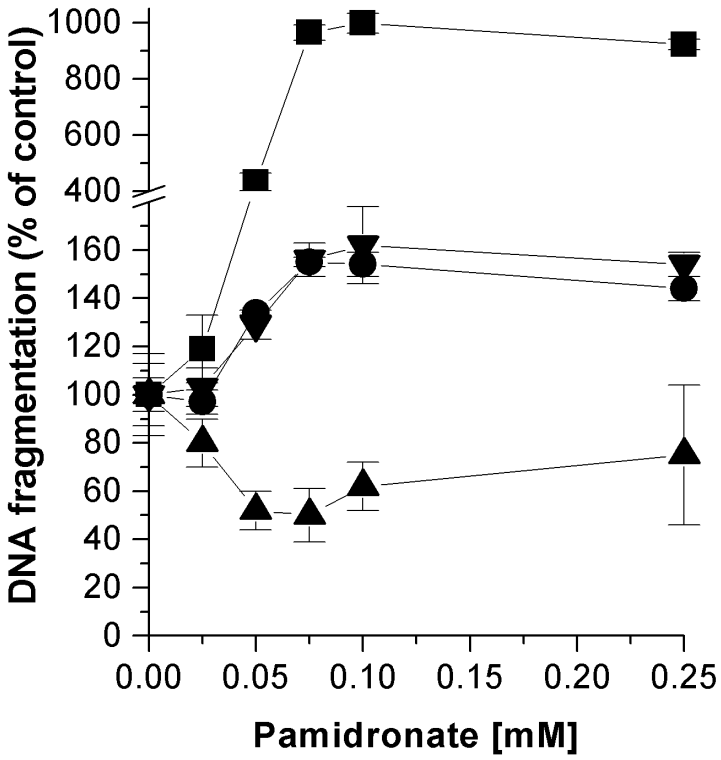

Figure 19:
Apoptosis of melanoma cells after pamidronate treatment. Melanoma cells of 80 % confluency were treated with indicated concentrations of pamidronate or vehicle control for 24 h. Apoptosis was measured as cytosolic nucleosomes using a sandwich ELISA. Squares, A375; circles, M186; up triangles, Mel2A; down triangles, M221. Error bars represent the standard deviation for four independent experiments.

Activation of so-called executor caspases is a further step of the apoptotic cell death. Caspases are cysteine proteases that are expressed as inactive zymogens. After proteolytic processing they form heterotetrameric complexes of large and small fragments of two caspases. The processing is achieved autocatalytically by initiation caspases which further process the executor caspases. Proteolytic degradation of target proteins is then performed by these caspases. Caspase-3 processing and activation was examined by Western blot using anti caspase-3 antibodies which detect the proenzyme of $M_r = 32 \cdot 10^3$ and cleaved enzyme forms of $M_r = 20 \cdot 10^3$ and $M_r = 17 \cdot 10^3$. Melanoma cells of 80 % confluency were treated with pamidronate, vehicle control or the CD95-agonistic monoclonal antibody CH-11 as a positive control. Whole cell lysates were prepared and subjected to SDS-PAGE. Subsequently, the gels were transferred to nitrocellulose membranes and the membranes probed with anti caspase-3 antibodies. The resulting immunocomplexes were detected using chemiluminescence. After treatment with 100 μM pamidronate for 24 h bands corresponding to the cleaved forms of $M_r = 20 \cdot 10^3$ and $M_r = 17 \cdot 10^3$ are visible in A375, M186 and M221 but not in Mel2A melanoma cells (Fig. 20).

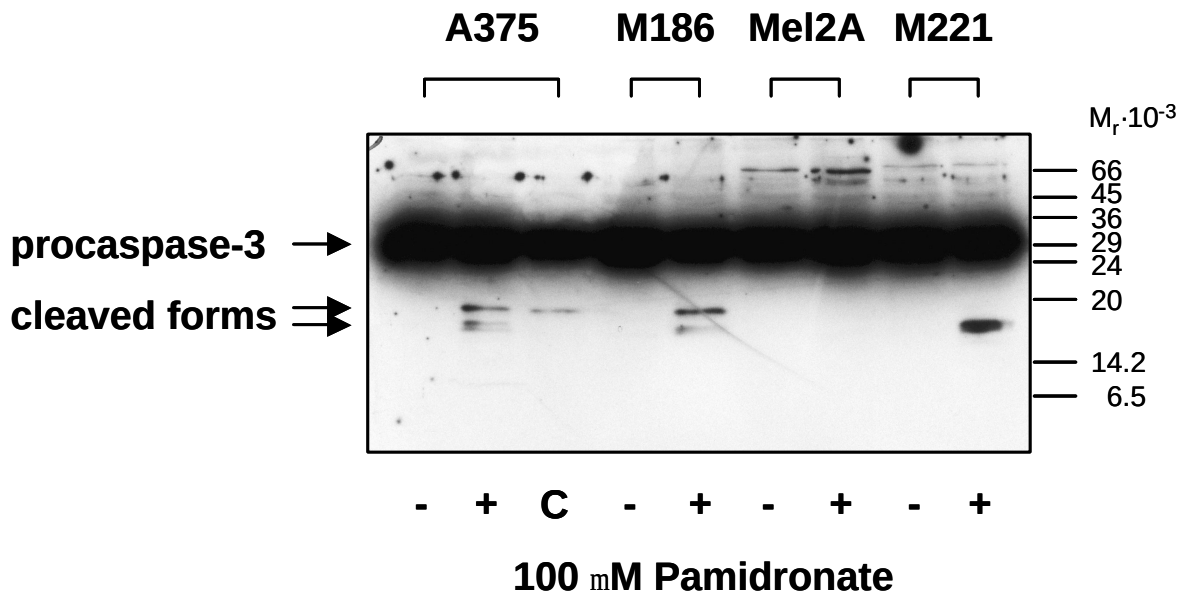

Figure 20:
Procaspase-3 cleavage upon pamidronate treatment in melanoma cells. Melanoma cells of 80 % confluency were treated with 100 μM pamidronate (+), vehicle control (-) or 1 μg/ml of the CD95-agonistic monoclonal antibody CH-11 (C) as a positive control for 24 h. Whole cell lysates were prepared and 50 μg of each were separated on a 15 % SDS-PAGE. After transfer to nitrocellulose the membrane was probed with anti caspase-3 antibodies. Immunocomplexes were detected using Super-Signal chemiluminescence reagent.

The most prominent effect of pamidronate is the inhibition of farnesyl diphosphate synthase (VAN BEEK *et al.*, 1999). Inhibition of this enzyme affects the synthesis of all higher isoprenoids. Whereas the synthesis of steroids via squalene is easily substituted by medium cholesterol, farnesylation of proteins or synthesis of geranylgeraniol and subsequent geranylgeranylation of proteins is decreased. Supplementation with farnesol or geranylgeraniol bypasses the effect of reduced isoprenylation of proteins. The addition of either farnesol or geranylgeraniol in the presence of pamidronate diminishes apoptosis in A375 cells in a concentration dependent manner (Fig. 21). Whereas 10 μM of either isoprenoid has no impact on pamidronat-induced apoptosis, farnesol at a concentration of 50 μM reduces the apoptotic effect of pamidronat by about 50 %. Geranylgeraniol at a concentration of 50 μM reduces the apoptotic effect of pamidronat by about 75 %. However, higher concentrations of 100 μM do not further decrease apoptosis and concentrations of 500 μM of either isoprenoid result in complete cell lysis.

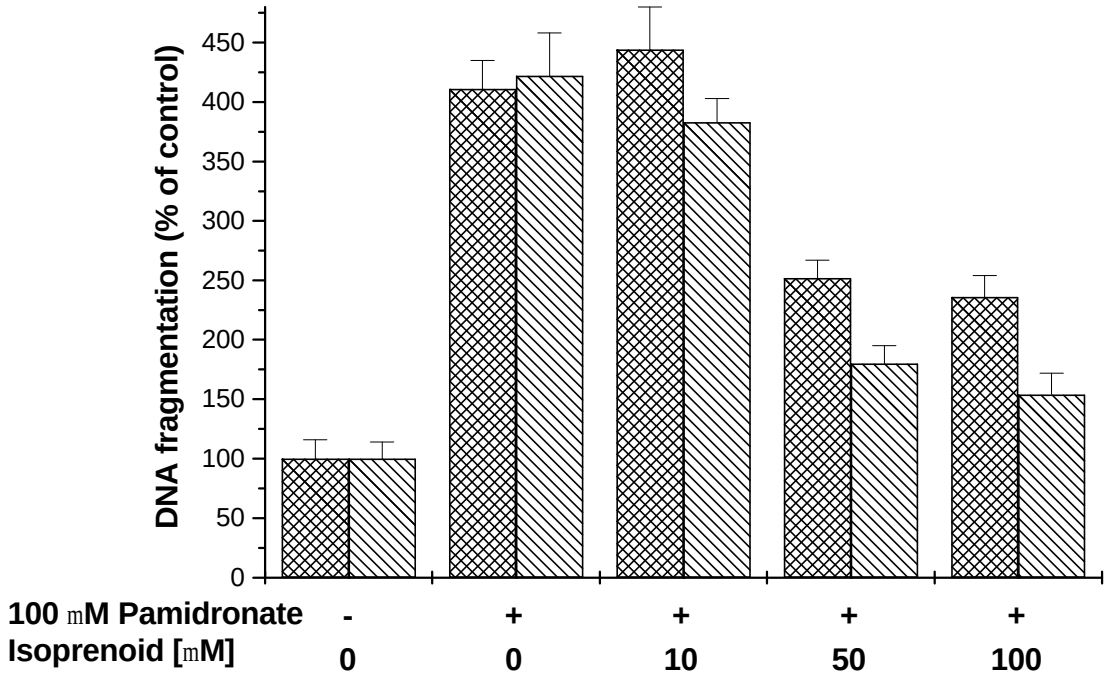

Figure 21:
Effect of isoprenoids on pamidronate-induced apoptosis in melanoma cells. A375 melanoma cells of 80 % confluency were treated with indicated concentrations of pamidronate and isoprenoids or vehicle control for 24 h. Apoptosis was measured as cytosolic nucleosomes using a sandwich ELISA. Crossed columns represent farnesol inclusion, hatched columns represent geranylgeraniol inclusion as indicated. Error bars represent the standard deviation for four independent experiments.

Shifting the ratio of the proapoptotic protein bax and the antiapoptotic protein bcl-2 is a mechanism how about 50 % of melanoma cells escape the immune system and achieve resistance against drugs entering the mitochondrial apoptotic pathway (RAISOVA *et al.*, 2001a). This resistance can be mimicked in cell culture by ectopic overexpression of bcl-2. A375 cells stably overexpressing murine bcl-2α and A375 transfected with vector only are equally sensitive to pamidronate-induced apoptosis (Fig. 22).

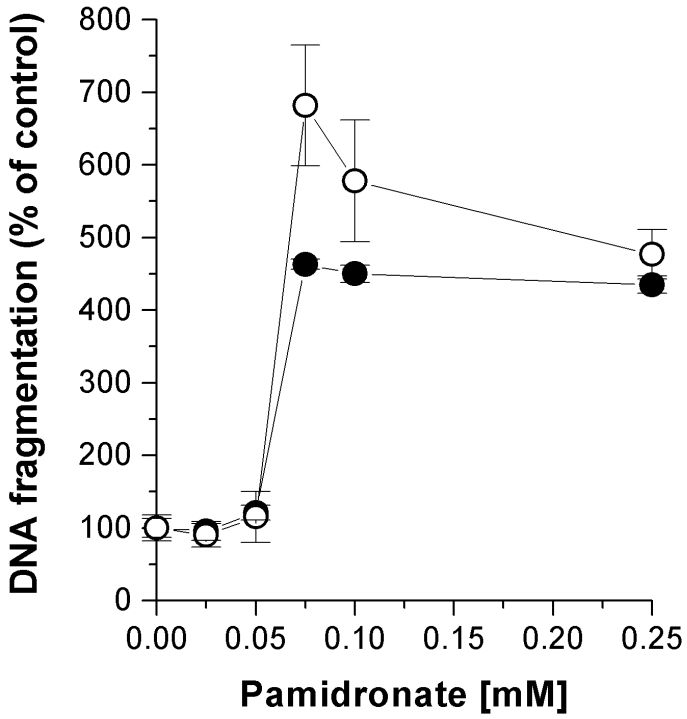

Figure 22:
Apoptosis of bcl-2 overexpressing melanoma cells after pamidronate treatment. Melanoma cells of 80 % confluency were treated with indicated concentrations of pamidronate or vehicle control for 24 h. Apoptosis was measured as cytosolic nucleosomes using a sandwich ELISA. Solid circles represent vector controls, open circles represent bcl-2 overexpressing A375 cells. Error bars represent the standard deviation for four independent experiments.

To investigate the expression of Rho isoforms in melanoma cells and primary cultured melanocytes, total RNA was isolated from post confluent grown cells. Synthesis of cDNA with 2 µg of total RNA was followed by PCR using specific primers under appropriate conditions (see chapter 5.6). Full-length coding sequence encompassing primers were designed and protocols optimised as described in chapter 2.2. Figure 23 shows the reaction products separated on 2 % agarose gels stained with ethidium bromide and scanned using video densitometry.

Whereas *RhoB* is heterogeneously expressed with M186, Mel2A and the primary melanocytes 02B1 showing strong expression, the expression of *rhoA* and *rhoC* is high in melanoma cells and low in melanocytes. The expression of *ribosomal protein S9* was included to show that comparable amounts of RNA were used.

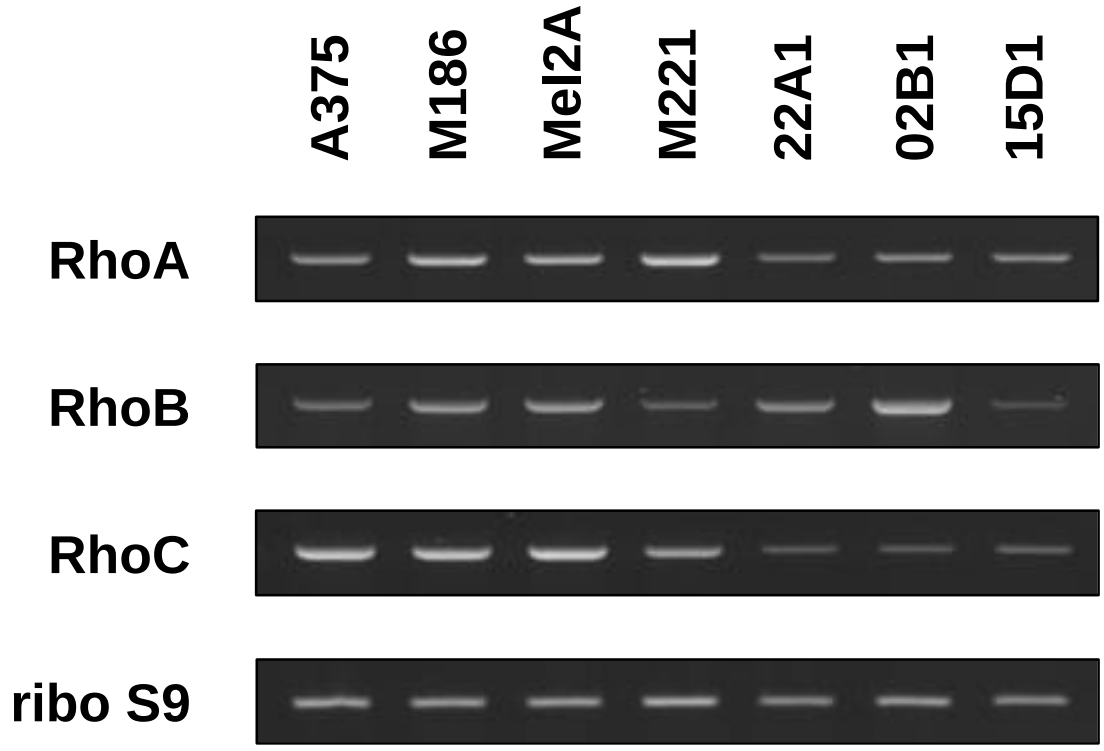

Figure 23:
Expression of Rho isoforms in melanoma cells and melanocytes. Total RNA was isolated from post confluent grown cells, cDNA synthesis with 2 μg of RNA performed and PCR with primers specific for the indicated mRNA was carried out. PCR products, 10 μl each were separated on 2 % agarose gels and visualised using ethidium bromide staining. ribo S9, ribosomal protein S9. A375, M186, Mel2A and M221 are melanoma cells; 22A1, 02B1 and 15D1 were primary cultured melanocytes.

The impact of pamidronate on Rho family proteins was analysed by investigation of the membrane localisation of RhoA as a representative by Western blot. To this end, melanoma cells were treated with vehicle control or 100 μM pamidronate for 24 h or 48 h. Whole cell lysates were prepared and centrifuged at 100,000 ×g for 1 h at 4 °C. Supernatants, representing the cytosol and pellets, representing the membrane fraction were subjected to SDS-PAGE. Subsequently, the gels were transferred to nitrocellulose membranes and the membranes probed with anti RhoA antibodies. The resulting immunocomplexes were detected using chemiluminescence.

The RhoA content of the cytosol increased after pamidronate treatment for 24 h and 48 h in the four melanoma cell lines tested (Fig. 24). Membrane-bound RhoA levels were unchanged in M186 and Mel2A after 24 h of treatment and in M186 after 48 h of treatment. Decreased RhoA levels were observed in membrane fractions of M221 after 24 h of treatment and in A375, Mel2A and M221 after 48 h of treatment.

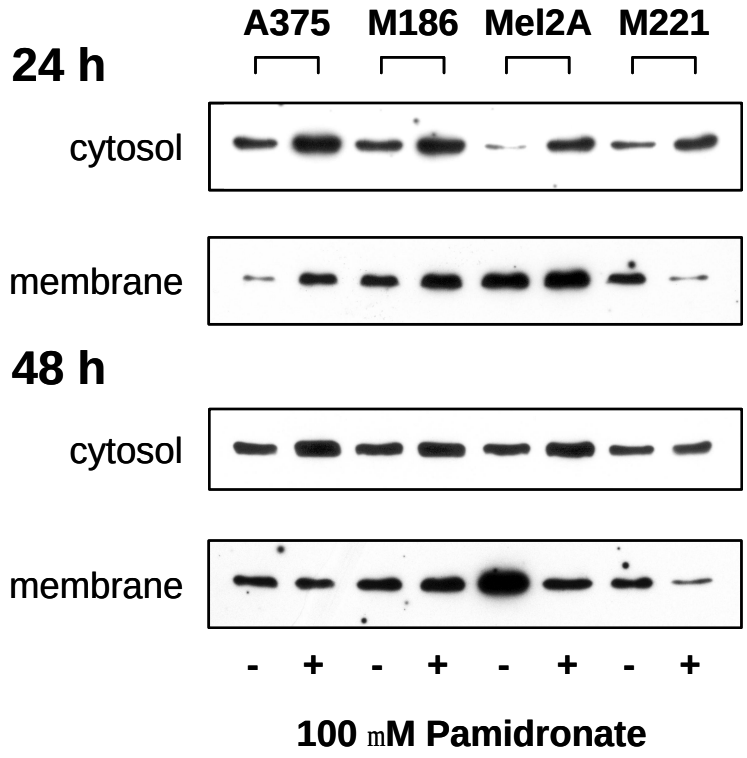

Figure 24:
Effect of pamidronate treatment on the subcellular distribution of RhoA. Cells were treated with vehicle control (-) or 100 µM pamidronate (+) for 24 h or 48 h as indicated. Cytosolic and membrane fractions were prepared by centrifugation of postnuclear supernatants at 100,000 ×g. Of the supernatants (cytosol), 50 µg protein and 150 µg protein of the resuspended pellet (membrane) were separated by 15 % SDS-PAGE. After transfer to nitrocellulose the membrane was probed with anti RhoA antibodies. Immunocomplexes were detected using SuperSignal chemiluminescence reagent.